OXFORD

ORIGINAL ARTICLE

Nogo Receptor 1 Limits Ocular Dominance Plasticity but not Turnover of Axonal Boutons in a Model of Amblyopia

Michael G. Frantz, Ryan J. Kast, Hilary M. Dorton, Katherine S. Chapman, and Aaron W. McGee

Developmental Neuroscience Program, Saban Research Institute, Children's Hospital Los Angeles, Department of Pediatrics, Keck School of Medicine, University of Southern California, Los Angeles, CA 90027, USA

Address correspondence to Aaron W. McGee, 4650 W Sunset Blvd, mailstop 135, Los Angeles, CA 90027, USA. Email: amcgee@usc.edu

Abstract

The formation and stability of dendritic spines on excitatory cortical neurons are correlated with adult visual plasticity, yet how the formation, loss, and stability of postsynaptic spines register with that of presynaptic axonal varicosities is unknown. Monocular deprivation has been demonstrated to increase the rate of formation of dendritic spines in visual cortex. However, we find that monocular deprivation does not alter the dynamics of intracortical axonal boutons in visual cortex of either adult wild-type (WT) mice or adult NgR1 mutant (*ngr1*–/–) mice that retain critical period visual plasticity. Restoring normal vision for a week following long-term monocular deprivation (LTMD), a model of amblyopia, partially restores ocular dominance (OD) in WT and *ngr1*–/– mice but does not alter the formation or stability of axonal boutons. Both WT and *ngr1*–/– mice displayed a rapid return of normal OD within 8 days after LTMD as measured with optical imaging of intrinsic signals. In contrast, single-unit recordings revealed that *ngr1*–/– exhibited greater recovery of OD by 8 days post-LTMD. Our findings support a model of structural plasticity in which changes in synaptic connectivity are largely postsynaptic. In contrast, axonal boutons appear to be stable during changes in cortical circuit function.

Key words: axon, bouton, electrophysiology, in vivo imaging, long-term monocular deprivation, optical imaging

Introduction

In the mammalian neocortex, most excitatory synapses reside on dendritic spines, small protrusions from the dendritic shaft that contain a postsynaptic density (Sala and Segal 2014). The corresponding presynaptic apparatus harboring synaptic vesicles often forms a varicosity, or bouton, on the axon (Debanne et al. 2011). Several studies have correlated the rate of formation, loss, and stability of dendritic spines with experience-dependent plasticity in sensory cortex (Holtmaat and Svoboda 2009). These imaging experiments have focused almost exclusively on dendritic spines of apical dendrites present in layer I of layer V pyramidal neurons, and to a lesser extent II/III pyramidal neurons. Spine dynamics are altered in somatosensory barrel cortex by several manipulations that affect the size of receptive fields for associated whiskers, including chessboard deprivation (Trachtenberg et al. 2002). Similarly, inducing abnormal vision by closing one eye (monocular deprivation, MD) alters eye dominance and increases spine formation and stability in the binocular zone of visual cortex of adult mice (Sawtell et al. 2003; Fischer et al. 2007; Sato and Stryker 2008; Hofer et al. 2009; Sala and Segal 2014). However, while the turnover of axonal boutons is lower than that of dendritic spines (De Paola et al. 2006; Debanne et al. 2011), whether the dynamics of these presynaptic structures present in layer I are also responsive to sensory manipulation or correlated with experience-dependent plasticity is unknown.

Ocular dominance (OD) plasticity is a premier model of experience-dependent plasticity (Morishita and Hensch 2008; Holtmaat and Svoboda 2009). The developing visual system is acutely sensitive to the quality of visual experience during a specified "critical period." In mice, this critical period extends from approximately postnatal days (P) 19 to 32 (Gordon and Stryker 1996; Trachtenberg et al. 2002). Monocular deprivation for a few days (3–5 days) during the critical period shifts the relative OD toward the nondeprived eye as a consequence of depression of visual responses to the deprived eye (Frenkel and Bear 2004; Sato and Stryker 2008). After the critical period, longer periods of MD (5–7 days) are required to induce an OD shift in adult mice (Sawtell et al. 2003; Sato and Stryker 2008). This adult OD shift results from a potentiation of nondeprived eye responses and correlates with increased spine formation and stability (Hofer et al. 2009). However, the magnitude of OD plasticity varies with the method of measurement. Adult OD plasticity is greater as measured with visually evoked potentials (VEPs) or optical imaging of intrinsic signals (OIS), 2 techniques that reflect a combination of subthreshold and suprathreshold neural activity, whereas plasticity is less evident with single-unit electrophysiological recordings that examine neuronal firing (Morishita and Hensch 2008).

MD lasting a few days induces a transient shift in OD whereas longer durations of MD (long-term MD, LTMD) initiated near the opening of the critical period results in both a permanent shift in OD toward the nondeprived eye and deficits in spatial vision by the deprived eye, including lower visual acuity (Mitchell and Sengpiel 2009). In mice, LTMD from P21 to P35 is sufficient to yield a maximum shift in OD (Gordon and Stryker 1996) and reduce visual acuity from the normal value of approximately 0.5 cycles per degree (cpd) to slightly more than 0.3 cpd. In behavioral tests of visual acuity, this impairment is permanent (Prusky and Douglas 2003).

Interestingly, mice lacking a functional gene for the neuronal nogo-66 receptor (*ngr1*) retain critical period OD plasticity as adults (McGee et al. 2005). These *ngr1* mutant mice (*ngr1*–/–) also spontaneously recover visual acuity following LTMD (Stephany et al. 2014). *Ngr1*–/– mice have been reported to exhibit greater dendritic spine and axonal bouton dynamics in both sensory and motor cortex (Akbik et al. 2013). However, while *ngr1* has been proposed to determine the low set point for synaptic structural plasticity in adult cortex, whether *ngr1* alters anatomical plasticity associated with experience-dependent cortical plasticity is not yet known.

To explore the correlation between OD plasticity and the dynamics of axonal boutons in visual cortex, first we examined the turnover and stability of axonal boutons in both adult WT and adult *ngr1*–/– mice during 8 days of MD. Next, we correlated the dynamics of axonal boutons following LTMD with 2 different measurements of OD plasticity, OIS, and single-unit recordings for both genotypes. *Ngr1*–/– mice displayed greater recovery of normal eye dominance but neither normal vision, MD, LTMD, nor binocular vision following LTMD altered the dynamics of axonal boutons in WT or *ngr1*–/– mice. We propose that *ngr1* limits cortical recovery from LTMD but does not restrict anatomical plasticity of axonal boutons in visual cortex.

Materials and Methods

Mice

All animal procedures were conducted under protocols reviewed and approved by the Children's Hospital Los Angeles Institutional Animal Care and Use Committee.

The constitutive *ngr1*–/– strain has been described previously (Kim et al. 2004). The *ngr1*–/– strain was F8 when this line was re-derived. The line was then backcrossed against C57Bl6 Thy1-EGFP-M transgenic mice (Feng et al. 2000), obtained from a commercial vendor (The Jackson Laboratory). Mice were group housed with same-sex littermates, and food and water were available *ad libitum*.

Cranial Windows for Repeated Imaging of Axonal Boutons in Visual Cortex

Male and female c57/Bl6 EGFP-M transgenic mice (postnatal (P) 45 and older) (transgenic line M; Jackson Laboratories) were used. Mice were anesthetized with isoflurane and administered dexamethasone (4 μg/g body weight) subcutaneously. Body temperature was maintained with a biofeedback heatpad (Physitemp). Cranial windows were implanted as previously described, with a minor modification (Holtmaat et al. 2009). A circular region of the skull over V1 visual cortex was removed without perturbing the underlying dura. A 2.5-mm diameter #1 thickness cover glass (Bellco) was placed on the dura, affixed with cyanoacrylate (Krazyglue), and sealed with dental acrylic. A small aluminum bar with tapped screw holes was embedded into the acrylic to stabilize the animal for subsequent imaging sessions. Mice received buprenorphine (0.1 μg/g body weight) for 3 days post-surgery and their water was supplemented with carprofen (1:2000) throughout the imaging series. Animals were given at least 2 weeks to recover before initiating imaging as cranial windows that were optically clear at 2 weeks were likely to remain clear for the duration of the experiment. Cranial windows were implanted between postnatal days 50 and 60. Two-photon imaging began between postnatal days 64 and 74.

Thinned Skull Cranial Window Preparation for Intrinsic Signal Imaging

Mice were anesthetized with isoflurane and administered dexamethasone (4 μg/g body weight) subcutaneously. Body temperature was maintained with a biofeedback heatpad (Physitemp). A circular region of the skull over V1 visual cortex was thinned and a 3.0-mm diameter #1 thickness cover glass (Bellco) was placed on the thinned bone, affixed with cyanoacrylate (Krazyglue), and sealed with dental acrylic. A small aluminum bar with tapped screw holes was embedded into the acrylic to stabilize the animal for subsequent imaging sessions. Animals received buprenorphine (0.1 μg/g body weight) for 3 days post-surgery, and their water was supplemented with carprofen (1:2000) throughout the imaging series. Animals were imaged starting 2–3 days post-surgery and then subsequently 2, 4, and 8 days later.

Monocular Deprivation

For 8-day MD, the eye contralateral to the hemisphere of study was closed using a single-mattress suture tied with 6–0 polypropylene monofilament (Prolene 8709H, Ethicon) under brief 1% isoflurane anesthesia. The knot was sealed with cyanoacrylate glue. For LTMD, the eye contralateral to the hemisphere of study was closed on P23. At the conclusion of LTMD, mice were again briefly anesthetized with isoflurane and the sutures cut away with fine iridectomy scissors. The eyelids were separated and the eye flushed with sterile saline solution. The eye was examined under a stereomicroscope, and mice with scarring of the cornea were eliminated from the study.

Optical Imaging of Intrinsic Signals

Imaging was performed as described previously (Cang et al. 2005; Kalatsky et al. 2005; Smith and Trachtenberg 2007; Sato and Stryker 2008). Mice were administered chlorprothixene (1 μg/g body weight; Sigma), and anesthesia was maintained with isoflurane. To visualize visually evoked changes in OIS in V1 visual cortex, horizontal bar 2 degrees high and 20 degrees wide descended from +40 to −40 degrees of the mouse's binocular visual field with a period of 8 s. This stimulus was repeated 35 consecutive times per experiment.

Green light (530 ± 30 nm) was used to visualize cerebral vascularization and red light (620 ± 20 nm) to image intrinsic signals. The imaging plane was focused ∼200–400 μm below the pial surface. Images were acquired at 10 frames per second at 1024 × 1024 pixels per image at 12-bit depth with a high-speed camera (Dalsa 1M60) and custom acquisition and analysis software (C++ and Matlab). Collected images were spatially binned before the response at the stimulus frequency was extracted from a complete time series for each pixel by Fourier analysis (Cang et al. 2005; Kalatsky et al. 2005).

To measure OD, vision was occluded for one eye during imaging with a removable eye patch constructed from electrical tape. At the end of each trial, the patch was switched to the other eye. Three or more trials were conducted for each eye. The magnitude of each trial was the average of the top 30% of pixel values within the region of response. Ocular dominance Index (ODI) was calculated by averaging these trials for each eye and dividing the difference of the contralateral (C) and ipsilateral (I) responses by their sum $(C − I)/(C + I)$.

Single-Unit Recordings

Recordings were adapted from our previously published methods and were performed by an investigator unaware of the genotype (McGee et al. 2005). Recordings were performed with Epoxylite-coated tungsten microelectrodes with tip resistances of 5–10 MΩ (FHC), amplifier (model 3600, A-M systems), and digitizer (micro1401, Cambridge Electronic Design) under Nembutal (50 mg/kg, i.p.; Abott)/chlorprothixene (10 mg/kg, i.m; Sigma) anesthesia. Atropine (20 mg/kg, s.c.; Sigma-Aldrich) was injected to reduce secretions and the parasympathetic effects of anesthetic agents, and dexamethasone (4 mg/kg, s.c.; American Reagent) was administered to reduce cerebral edema. Pure O_2 gas was blown over the nostrils at 1 L/min. A craniotomy was made over the left visual cortex, and agar was applied to enhance recording stability and prevent desiccation. The eyelids were removed from both eyes, and the corneas protected thereafter by frequent application of silicon oil. Animal temperature was maintained at 37°C by a homeostatically controlled heating pad. Heart rate and oxygen saturation were monitored continuously (Kent Scientific).

The electrophysiological responses for 4–6 cells separated by >90 μm in depth were recorded for each electrode penetration. In each mouse, 4 to 6 separate penetrations were spaced evenly at least 200 μm apart across the binocular region, defined by a receptive field azimuth of <25°. Responses were evoked with 0.1 cpd 95% contrast sinusoidal drifting gratings presented at 6 different orientations separated by 30° generated by custom software (Matlab). Gratings were presented for 2 s during a 4-s trial. A blank trial was also included during which no grating was presented. Each of these 7 stimuli (6 orientations and the blank) was presented 6 times in random order save that each orientation followed the blank stimuli only once. Action potentials (APs) were identified in recorded traces of neural activity with Spike2 (Cambridge Electronic Design). For each unit, APs were summed for each orientation. The orientation with the greatest number of APs was considered the preferred orientation. Cells in which the number of APs at the preferred orientation was not at least 50% greater than the blank were deemed nonresponsive and discarded.

Cells were assigned to OD categories according to the 7-category scheme of Wiesel and Hubel (1963). To categorize each unit, first the number of APs for the stimulus blank was subtracted from the average number of APs per stimuli provided to each eye. Next, the responses to the contralateral eye (C) and ipsilateral eye (I) were computed as follows: $(C − I)/(C + I)$ as described previously (Rittenhouse et al. 1999). This scalar was then binned into OD categories 1–7 as follows: 1 to 0.75 = 1, 0.75 to 0.45 = 2, 0.45 to 0.15 = 3, 0.15 to −0.15 = 4, −0.15 to −0.45 = 5, −0.45 to −0.75 = 6, and −0.75 to −1 = 7. To determine the contralateral bias index (CBI), the number of units in each category was summed for all mice in a group, and the CBI was calculated according to the formula: $CBI = [(n_1 − n_7) + (2/3)(n_2 − n_6) + (1/3)(n_3 − n_5) + N]/2N$, where N is the total number of units and n_x = number of units with OD scores equal to x (Gordon and Stryker 1996).

Laminar Analysis

Units were categorized as layer II/III, IV or V based on the depth of the electrode measured from the pial surface. Units recorded between 150 and 349 μm were classified as layer II/III, units between 350 and 499 μm were classified, and units between 500 and 700 μm were classified as layer V.

Chronic In Vivo Two-Photon Imaging

All imaging was conducted blind to the genotype. Animals were anesthetized with isoflurane, and body temperature was maintained with a biofeedback heatpad (Physitemp). Images were acquired with a modified Movable Objective Microscope (Sutter Instruments) and 40X 1.0 nA water immersion objective (Zeiss) using scanimage software (MatLab) (Pologruto et al. 2003). The light source is a Ti:sapphire tunable laser (Chameleon Ultra II, Coherent) operating at 910 nm. Imaging typically required less than 50 mW of power. Image stacks consisted of sections (512 × 512 pixels) collected in 1-μm steps. Low-magnification images (0.56 μm/pixel) were taken to visualize axonal arbors. These guided the high-magnification images (0.14 μm/pixel) collected for bouton analysis. Care was taken to maintain the same level of fluorescence across imaging intervals. Animals were imaged every 4 days. Imaging sessions lasted no more than 2 h. All images of neuronal structures presented in this study are best projections from z-stacks after linear contrast adjustment (Image J, NIH and Photoshop software, Adobe).

Image Analysis for Axonal Boutons

Boutons were identified and image analysis performed following published guidelines (De Paola et al. 2006). Boutons were defined as new if they were 3 times brighter than the surrounding axon and lost if their fluorescence decreased to lower than 1.3 times the surrounding axon. All analysis was done blind to genotype using ImageJ (NIH). Clearly defined boutons present on axons in the first imaging interval were labeled in ImageJ. In image stacks from subsequent imaging sessions, experimenters determined whether a labeled bouton was still present or not and checked for the appearance of new boutons. Newly added

boutons were also tracked throughout subsequent imaging sessions. An experimenter blind to genotype analyzed the image stack series for each field. In the case of a discrepancy between the 2 sets of analysis, a third experimenter repeated the analysis.

Statistics

Statistical comparisons were performed with Prism software (GraphPad). All values are reported at the mean ± standard error of the mean (SEM). The rates of addition and loss of axonal boutons were compared with the Kruskal–Wallis test followed by Dunn's multiple comparison test (unless otherwise noted) as the n for these experiments is too small to confirm a normal distribution. The recovery of OD by OIS was compared between genotypes by repeated-measures two-way ANOVA with Bonferroni correction for multiple comparisons. Comparisons of WT and *ngr1–/–* ODI values at different times post-LTMD were compared with the ODI of naïve mice with the Kruskal–Wallis test followed by Dunn's multiple comparison test. Electrophysiological measurements of OD were compared between genotypes using the Mann–Whitney test. The distributions of OD indices of single units were compared between genotypes using the Kolmogorov–Smirnov (KS) test.

Results

Axonal Boutons Maintain Normal Dynamics during MD

MD alters dendritic spine density both during the critical period for OD plasticity and in adulthood (Mataga et al. 2004; Hofer et al. 2009; Djurisic et al. 2013). In adult mice, 4 days of MD doubles the rate of spine addition in layer I in the binocular zone of primary visual cortex but does not alter the rate of spine elimination (Hofer et al. 2009). To test whether axonal boutons in layer I exhibit similar sensitivity to abnormal visual experience, we repeatedly imaged axonal structures every 4 days before and during MD in adult WT and *ngr1–/–* mice harboring the EGFP-M transgene (Feng et al. 2000) (Fig. 1).

We employed OIS to identify the binocular zone of primary visual cortex for repeated two-photon imaging of axons (Fig. 1A). This imaging approach extracts the cortical response to a periodic stimulus by Fourier analysis and yields the magnitude of this response as the fractional change in reflectance specific to the frequency of the visual stimulus (ΔR/R) (Fig. 1B) (Kalatsky and Stryker 2003; Cang et al. 2005). The visual stimulus was presented in the central 20° of the visual field to both eyes to map the binocular zone for 8-day MD imaging experiments (Fig. 1C). The same stimulus was provided exclusively to the non-deprived eye ipsilateral to the cranial window for subsequent experiments examining axonal plasticity after LTMD (Fig. 1D). Low-magnification images of a field of axons imaged before and after a 4-day interval reveal that the clarity and contrast of these images were sufficient to reliably identify both axons and axonal boutons at multiple time points (Fig. 1E).

First, we imaged axonal boutons in the binocular zone of visual cortex of both WT and *ngr1–/–* mice for several consecutive 4-day intervals before MD and then during 8 days of MD (Fig. 2). The formation and loss of a small percentage of axonal boutons was evident over this imaging series (Fig. 2A). Prior to MD, the rates of bouton gain and loss were indistinguishable between WT and *ngr1–/–* mice (Fig. 2B,C). In contrast to dendritic spine dynamics, MD did not alter the rate of bouton addition for either WT or *ngr1–/–* mice (Fig. 2B). MD also did not alter the rate of bouton loss for either genotype (Fig. 2C). The stability of new boutons also was not statistically different. The percentage of new boutons that were present for a single imaging time point and categorized as "transient," versus boutons that were present for more than one imagine interval and considered "persistent," was similar between genotypes and not altered by MD (Fig. 2D).

Axonal Boutons Maintain Normal Dynamics during LTMD and following Restoration of Normal Vision

LTMD results in a permanent impairment of visual acuity in WT mice (Prusky and Douglas 2003). *Ngr1–/–* mice display low acuity
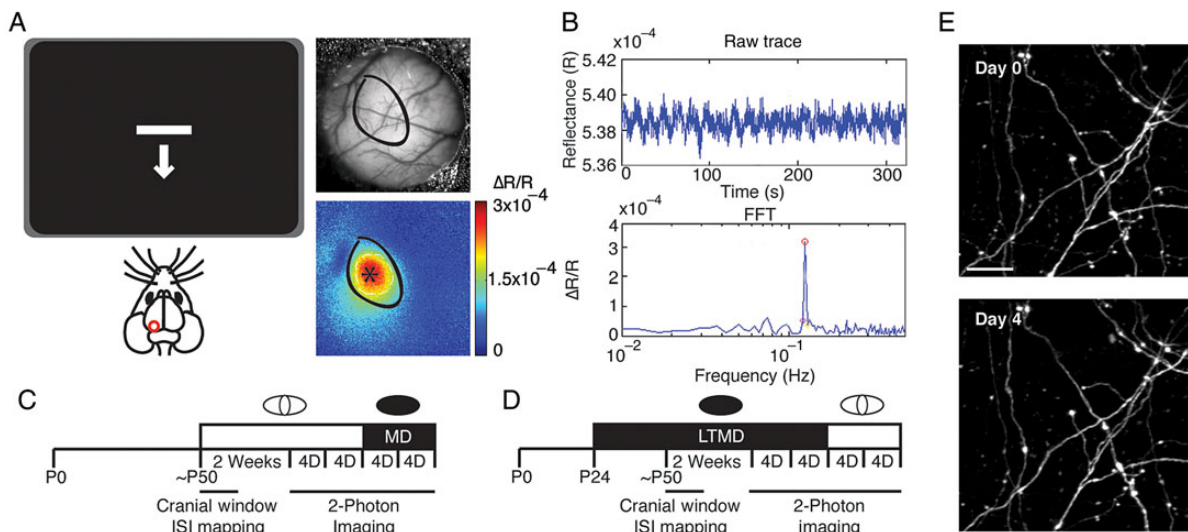

Figure 1. Experimental design (A) Schematic for the setup of OIS. The magnitude of the cortical responses (ΔR/R) to a drifting horizontal bar (left) is represented as false-color intensity map for each pixel (lower right). The region of response is circled. This corresponds to the binocular zone. Mapping this region onto the surface vasculature (upper right) identifies the location for chronic two-photon imaging of axonal structures in vivo relative to reference points of the vasculature. (B) (upper) An example trace of the changes in reflectance for one pixel located within the binocular zone during the presentation of the stimulus [pixel location is indicated by the asterisk in (A)]. Fourier analysis of this waveform extracts the magnitude (ΔR/R) of the neural response corresponding to the frequency of the visual stimulus. (C) Experimental timeline for examining axonal plasticity during MD. (D) Experimental timeline for examining axonal plasticity following LTMD. (E) A field of axons in the binocular zone imaged with two-photon microscopy at 2 time points, 4 days apart. Scale bar 15 μM.
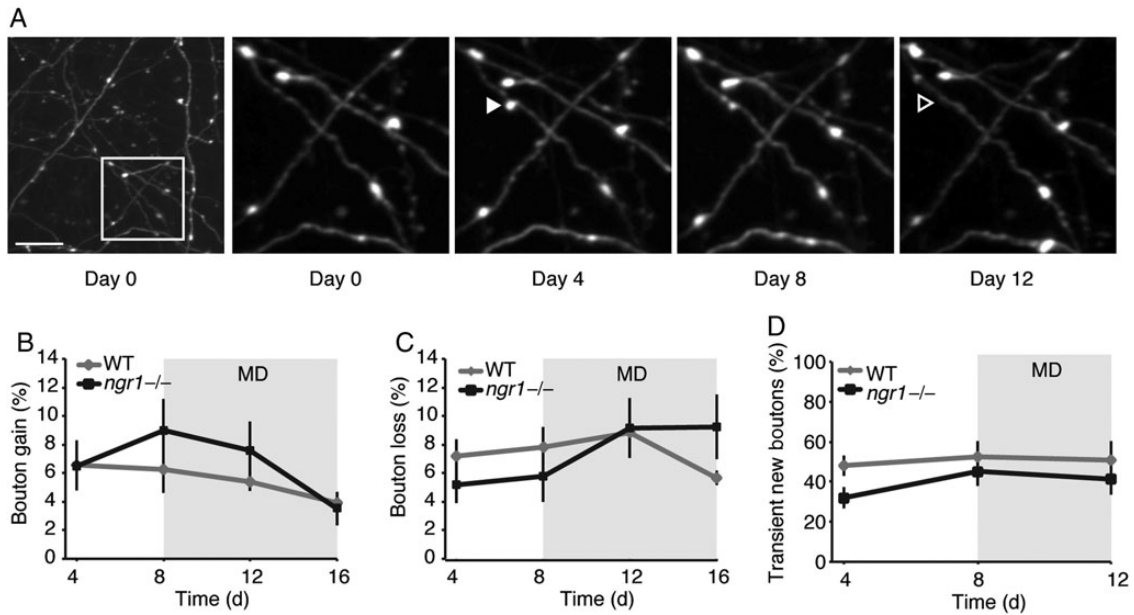
Figure 2. Turnover of axonal boutons in vivo during adult OD plasticity. (A) A field of axons over a 12-day imaging time course. Left, a lower magnification view is presented. Right, segments of axons repeatedly imaged at 4-day intervals. Filled triangles indicate boutons gained and open triangles indicate boutons lost. (B) The percentage of boutons gained for each genotype during 2 baseline imaging sessions (Days 4 and 8) were indistinguishable (WT 4 mice, 1278 boutons; $ngr1-/-$ 6 mice, 1253 boutons) (gained Pre-MD, WT $6.4 \pm 1.1\%$, $n = 4$, $ngr1-/-$ $7.7 \pm 1.1\%$, $n = 6$, $P > 0.9$). The rate of bouton gain was similar before (Days 4 and 8) during MD (Days 12 and 16) (WT, pre-MD, $6.4 \pm 1.1\%$, 4-day MD, $5.4 \pm 0.6\%$, $P > 0.9$; $ngr1-/-$, pre-MD, $7.7 \pm 1.1\%$, 4-day MD, $7.6 \pm 1.7\%$, $P > 0.9$) (C) The percentage of boutons lost for each genotype during were similar both during 2 baseline imaging sessions (Days 4 and 8) and MD (Days 12 and 16) (WT 4 mice, $ngr1-/-$ 6 mice, lost, WT $7.5 \pm 0.9\%$, $n = 4$, $ngr1-/-$ $5.5 \pm 0.9\%$, $n = 6$, $P > 0.9$; WT, pre-MD, $7.5 \pm 0.9\%$, 4-day MD, $8.8 \pm 1.7\%$, $P > 0.9$; $ngr1-/-$, pre-MD, $5.5 \pm 0.9\%$, 4-day MD, $9.1 \pm 1.7\%$, $P > 0.25$) (D) The percentage of new boutons that were transient and present for only one imaging session was similar between genotypes and conditions (WT vs. $ngr1-/-$; $P > 0.13$, pre-MD vs. post-MD, $P > 0.30$). Overall, there were no significant differences between the rates of bouton gain or loss across genotype or condition. Statistical comparisons within and between genotypes and conditions were performed with the Kruskal–Wallis test and Dunn's correction for multiple comparisons.

similar to WT mice in the week following restoration of normal vision but then exhibit spontaneous improvement in visual acuity over the next 6 weeks (Stephany et al. 2014). To test whether the dynamics of axonal boutons in layer I are altered by the restoration of normal vision in adulthood after LTMD in either WT or $ngr1-/-$ mice, we imaged axons in the binocular zone of primary visual cortex contralateral to the deprived eye for several 4-day intervals during and after LTMD (Fig. 3). There was no difference between WT and $ngr1-/-$ mice in the rate of addition of axonal boutons during LTMD (Fig. 3A). The rate of bouton loss in WT and $ngr1-/-$ was also similar (Fig. 3B). Reopening of the deprived eye after approximately 6 weeks of LTMD did not alter the rate of bouton addition for either genotype but did increase the variability in the rate of bouton loss. This resulted in a trend toward greater bouton loss in the 4 days following eye re-opening, but this difference did not achieve statistical significance (Fig. 3B). In contrast to the effects of MD on OD and dendritic spine dynamics, presynaptic structural plasticity by putative intracortical axons was not altered by either MD or restoration of vision following LTMD (Fig. 3A–D).

WT and $ngr1-/-$ Mice Recover Normal Contralateral Bias Rapidly following LTMD as Assessed with OIS

Improvement in visual acuity in $ngr1-/-$ mice by the previously deprived eye following LTMD requires several weeks of subsequent normal vision. To examine the acute response of primary visual cortex to restoration of vision after LTMD in WT and $ngr1-/-$ mice, we performed chronic OIS to measure OD in the binocular visual cortex from immediately following re-opening the deprived eye to 8 days thereafter (Fig. 4). The relative strength

of the cortical response to the same visual stimulus provided to the contralateral eye (C) and ipsilateral eye (I) is reported as the $ODI = (C - I)/(C + I)$ (Cang et al. 2005). After re-opening the contralateral eye under isoflurane anesthesia, responses to a visual stimulus presented to this eye were barely detectable in both genotypes of mice, yielding is a negative ODI (Fig. 4A,B). Surprisingly, both WT and $ngr1-/-$ rapidly recovered normal contralateral bias in 4–8 days.

After 2 days of normal vision, both WT and $ngr1-/-$ mice had recovered significant cortical responsiveness to visual stimulation through the contralateral eye but the average ODI remained significantly more binocular than naïve mice (Fig. 4B,C). By 4 days post-LTMD, the ODI of WT mice was similar to that of naïve mice, and while the recovery of $ngr1-/-$ mice slightly less, the responses to visual stimulation of the ipsilateral eye decreased for both genotypes (Fig. 4B,D). By 8 days post-LTMD, both WT and $ngr1-/-$ mice were indistinguishable from naïve mice (Fig. 4B).

NgR1–/– Mice Exhibit Recovery of OD by Single-Unit Recording after LTMD

As hemodynamic measures of OD identify plasticity not detected with classical single-unit electrophysiological recording (Morishita and Hensch 2008), we investigated whether $ngr1-/-$ mice display OD plasticity after LTMD sufficient to restore neuronal firing activity as well (Fig. 5). We performed single-unit recordings on WT and $ngr1-/-$ mice receiving LTMD throughout the critical period and maintained for 6 weeks until the day of the experiment (Day 0) or after 8 days of normal vision (Day 8) (Fig. 5A). On Day 0, the OD histograms (Fig. 5B), the mean of CBI reflecting
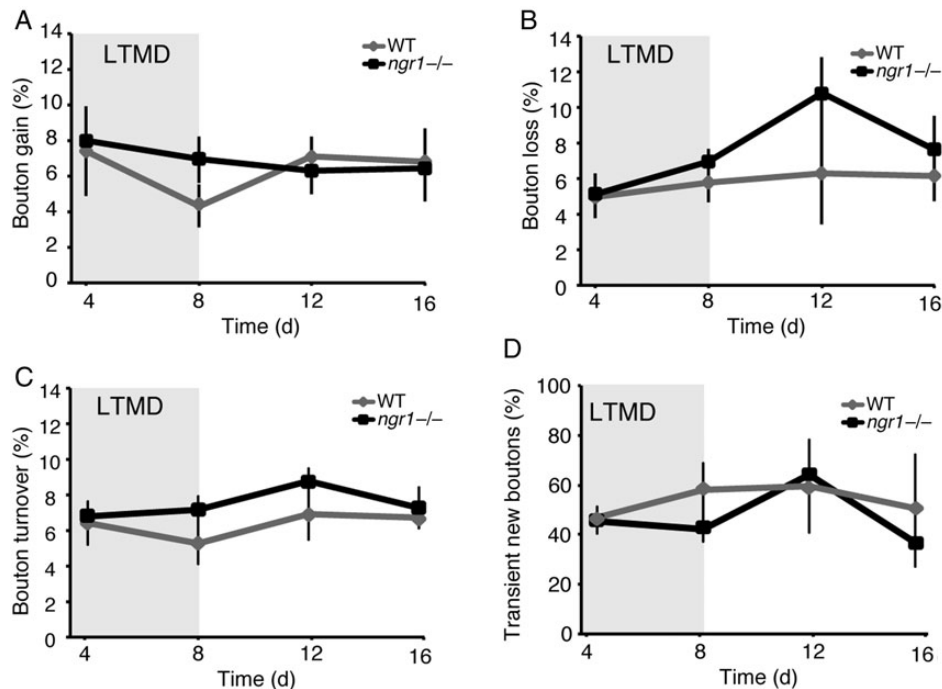
Figure 3. Turnover of axonal boutons in vivo during recovery from LTMD. (A) The percentage of boutons gained for WT and *ngr1*–/– mice during LTMD (Days 4 and 8) and during 8 days of subsequent binocular vision (Days 12 and 16) (WT 4 mice, 727 boutons; *ngr1*–/– 6 mice, 1411 boutons). Bouton gains were similar between genotypes and conditions (gains, WT, LTMD, 7.7 ± 0.9% vs. 4-day vision, 6.7 ± 1.3%, $n = 4$, $P > 0.9$; *ngr1*–/–, LTMD, 7.5 ± 0.8% vs. 4-day vision, 6.3 ± 1.2%, $n = 6$, $P > 0.9$) (B) The percentage of boutons lost for each genotype during LTMD (Days 4 and 8) and during 8 days of subsequent binocular vision (Days 12 and 16). There was a trend toward increased bouton loss during the first interval after eye opening, but it did not reach statistical significance due to increased variability in the rate of bouton loss (lost, WT, LTMD, 5.4 ± 0.8% vs. 4-day vision, 6.3 ± 3.4%, $n = 4$, $P > 0.9$; *ngr1*–/–, LTMD, 6.0 ± 0.6% vs. 4-day vision, 10.8 ± 2.0%, $n = 6$, $P > 0.09$). (C) Turnover of axonal boutons for WT and *ngr1*–/– mice. (D) The percentage of new boutons that were transient and present for only one imaging session was similar between genotypes and conditions. Statistical comparisons within and between genotypes and conditions were performed with the Kruskal–Wallis test and Dunn's correction for multiple comparisons.

the overall distribution of the eye dominance of single-unit activity summed across all layers of cortex for each mouse (Fig. 5C), and the cumulative distribution of ODI values each (Fig. 5D), revealed that WT and *ngr1*–/– mice both lack normal contralateral bias as a result of LTMD. This deficit was similar between genotypes (Fig. 5B–D) and corresponds to the maximal shift observed with 14 days of LTMD in preceding studies (Gordon and Stryker 1996). However, 8 days after the restoration of normal vision, WT displayed a modest but statistically significant shift toward binocularity. *Ngr1*–/– mice exhibited greater OD plasticity yielding a larger OD shift back toward the previously deprived contralateral eye. The OD shift at Day 8 was significantly greater in *ngr1*–/– mice (Fig. 5E). We conclude that although modest OD plasticity is detectable in adult WT mice with single-unit recordings following LTMD, OD plasticity is greater in *ngr1*–/– mice.

To characterize which layers within visual cortex displayed OD plasticity following LTMD in both WT and *ngr1*–/– mice, we categorized our single-unit recordings by depth from the pial surface into layer II/III (100–350 μm), layer IV (350–500 μm), and layer V (500–700 μm) and generated both OD histograms and cumulative distributions of these single-unit responses (Fig. 6). In WT mice, OD plasticity largely resulted from a decrease in units strongly favoring the ipsilateral eye (Categories 6 and 7) and an increase in units with binocular responses (Category 4) (Fig. 6A). By comparison, *ngr1*–/– mice at 8 days post-LTMD displayed an increase in the percentage of units with greater responses to the previously deprived contralateral eye (Categories 1–3) (Fig. 6A). This greater OD plasticity was more pronounced in the extragranular of visual cortex, layers II/III, and V, but was also

detectable in layer IV. Cumulative distribution histograms reveal that at 8 days post-LTMD *ngr1*–/– possess more units with ODI scores greater than zero that correspond to increasing contralateral bias in the extragranular layers (Fig. 6B).

Discussion

OD in primary visual cortex is a valuable model of how experience modifies functional and anatomical connectivity in the mammalian CNS. This plasticity is most prominent during a developmental critical period (Levelt and Hübener 2012). Within the critical period, short durations of MD shift the relative responsiveness of cortical neurons toward the nondeprived eye. However, these shifts in OD are rapidly corrected by restoring normal vision during the critical period, even if for only brief periods of time (Schwarzkopf et al. 2007). In contrast, LTMD throughout the critical period results in a permanent shift in OD and a sustained deficit in visual acuity (Morishita and Hensch 2008).

OD plasticity both in the critical period and in the adult is accompanied by anatomical plasticity. An immunohistochemical study reported that brief MD during the critical period results in a transient decrease in the density of synapses formed by thalamocortical axons originating from the lateral geniculate nucleus (LGN) (Coleman et al. 2010). By comparison, LTMD yields modest alterations in the length and extent of branch by thalamocortical arbors for both the deprived and nondeprived eye (Antonini et al. 1999). Postsynaptically, both MD and LTMD during the critical period alter spine density on pyramidal neurons (Mataga et al. 2004; Montey and Quinlan 2011; Djurisic et al. 2013), whereas
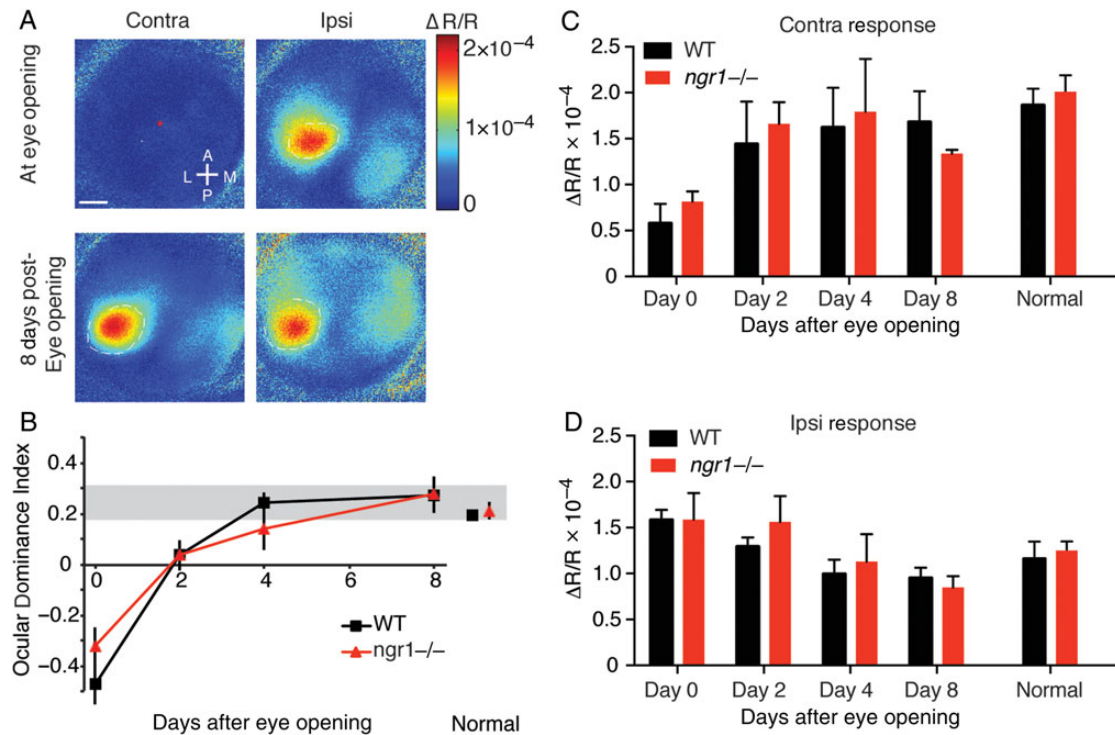
Figure 4. OD plasticity measured with repeated OIS following LTMD. (A) An example of response magnitude maps for the contralateral (contra) or ipsilateral (ipsi) eye for a WT mouse at eye opening and after 8 days binocular vision. Anterior (A), posterior (P), lateral (M), and medial (M) orientation of the image are indicated. Scale bar = 0.4 mm (B) Average ODI values for nondeprived (normal) WT and *ngr1*–/– mice and WT and *ngr1*–/– mice post-LTMD at eye opening and following 2,4, and 8 days of binocular vision, as well the average ODI of nondeprived WT and *ngr1*–/– mice. The gray bar represents the range of ODI values typical adult nondeprived WT ($n = 4$) and *ngr1*–/– mice ($n = 4$). Each mouse was imaged at each time point. The trajectory of recovery of OD in WT and *ngr1*–/– mice are similar (WT, $n = 4$, 2 days post-LTMD 0.04 ± 0.06 vs. nondeprived 0.20 ± 0.01, $P < 0.02$; *ngr1*–/–, $n = 4$, 2 days post-LTMD 0.04 ± 0.02 vs. nondeprived 0.20 ± 0.01, $P < 0.01$; WT, 4 days post-LTMD 0.25 ± 0.04 vs. nondeprived 0.20 ± 0.01, $P > 0.9$; *ngr1*–/–, 4 days post-LTMD 0.28 ± 0.04 vs. nondeprived 0.20 ± 0.01, $P > 0.8$; WT, 8 days post-LTMD 0.28 ± 0.07 vs. nondeprived 0.20 ± 0.01, $P > 0.9$; *ngr1*–/–, 8 days post-LTMD 0.28 ± 0.04 vs. nondeprived 0.20 ± 0.01, $P > 0.8$; Kruskal–Wallis test followed by Dunn's multiple comparison test) (C). The average magnitude of response to a visual stimulus presented to the contralateral eye of nondeprived WT and *ngr1*–/– mice, at eye-opening and after 2, 4, and 8 days of binocular vision following LTMD. (D) The average magnitude of responses to a visual stimulus presented to the ipsilateral eye of nondeprived WT and *ngr1*–/– mice, at eye-opening and after 2, 4, and 8 days of binocular vision following LTMD.

adult MD increases the rate of spine formation and stability of dendritic spines in layer I (Hofer et al. 2009).

Here, we measured the turnover of axonal boutons in layer I with chronic two-photon in vivo imaging. These axons possessed morphologies consistent with intracortical axons originating from layer II/III and layer V pyramidal neurons (De Paola et al. 2006) and likely originate from neurons both within and outside of visual cortex (Douglas and Martin 2004). In contrast to dendritic spines in layer I, the formation, loss, and stability of axonal boutons were unaffected by MD in WT mice (Figs 2 and 3). Thus, in WT mice, putative intracortical axonal boutons did not display the increase in the formation and stability observed by adjacent dendritic spines.

NgR1 binds to several potential inhibitors of synaptic structural plasticity, including some chondroitin sulfate proteoglycans (CSGPs) and proteins associated with myelin membranes, including Nogo-A (reticulon 4a, RTN4a), myelin-associated glycoprotein, and oligodendrocyte myelin glycoprotein (OMgp) (Mironova and Giger 2013). These myelin-associated inhibitors also bind to other receptors such as NgR2 and paired immunoglobulin-like receptor B (PirB) (Filbin 2008). Whether synaptic structural plasticity are altered in NgR2 or PirB mutant mice is not yet known.

Ngr1–/– mice have been reported to exhibit turnover rates in vivo for dendritic spines and axonal boutons in cerebral cortex

nearly triple that of WT mice (Akbik et al. 2013). This represents the largest increase in synaptic structural plasticity of age-matched mice for any environmental, pharmacologic, or genetic manipulation. We have also measured the turnover of dendritic spines in somatosensory barrel cortex of adult WT and *ngr1*–/– mice. In a recent study, we examined 3 times the number of spines per mouse over more consecutive time intervals than Akbik et al. (Park et al. 2014). However, in our experiments, dendritic spine turnover and stability were indistinguishable between WT and *ngr1*–/– mice.

Here, we measured the turnover of axonal boutons in functionally defined visual cortex both under baseline conditions and during MD. The rates of bouton addition and loss were also similar between WT and *ngr1*–/– mice. Akbik et al. imaged 541 boutons in total from 5 *ngr1*+/– mice and 510 boutons in total from 5 *ngr1*–/– mice across a single 14-day interval. In comparison, we examined 1278 boutons from 4 WT mice and 1253 boutons from 6 *ngr1*–/– mice across several 4-day intervals. Statistical analysis of our measurements of the baseline turnover rate for boutons prior to MD (Fig. 2) indicates that we would have detected a 40% increase in turnover by as significant ($P < 0.02$). Akbik et al. reported a nearly 150% increase in turnover. Although there are some technical differences between the 2 studies, both employed the same strain of *ngr1*–/– mice. Overall, given broad expression of *ngr1* in cerebral cortex combined with the
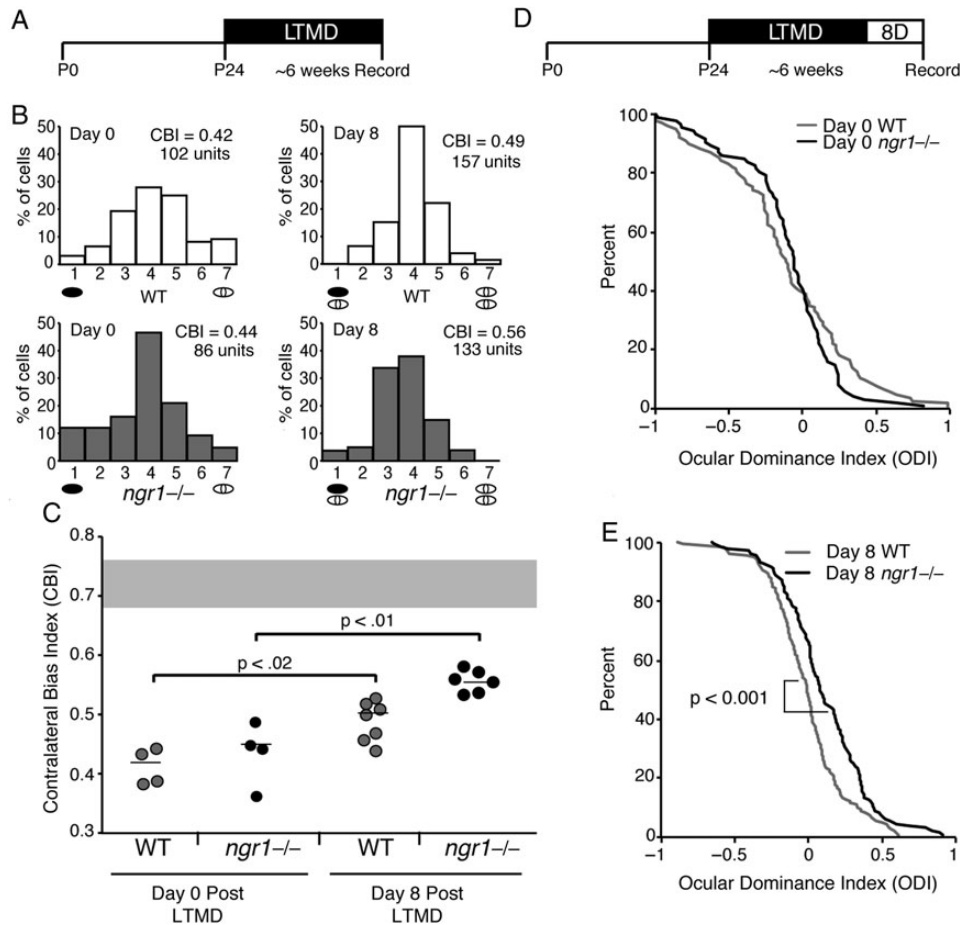
Figure 5. OD plasticity measured with single-unit recordings following LTMD. (A) Schematic of the experimental design. Mice were deprived of vision in the eye contralateral to the hemisphere of recording at P24. Several weeks later, single-unit recordings were performed on either during LTMD (Day 0) by opening the eye under anesthesia (left) or 8 days after the restoration of normal vision (right). (B) OD histograms for WT mice (top) and *ngr1–/–* mice (bottom) at Day 0, the time of eye opening (left), and after 8 days after re-opening the deprived eye (right). (C) CBI values for each mouse (circles). The horizontal line indicates the mean CBI value for the group. At eye opening after LTMD, both WT and *ngr1–/–* mice possessed minor ipsilateral eye dominance (CBI < 0.5). WT mice displayed a modest but statistically significant increase in CBI (WT, Day 0 CBI = 0.42 ± 0.02, $n = 4$ vs. Day 8 CBI = 0.49 ± 0.01, $n = 6$, $P < 0.02$, Mann–Whitney test) whereas *ngr1–/–* exhibited greater OD plasticity and higher CBI values (*ngr1–/–*, Day 0 CBI = 0.44 ± 0.03, $n = 4$ vs. *ngr1–/–*, Day 8 CBI = 0.56 ± 0.01, $n = 7$; $P < 0.01$, Mann–Whitney test). (D) Cumulative distributions of ODIs of individual units on the day of eye opening (Day 0) for WT and *ngr1–/–* mice are similar ($P > 0.4$, K–S test of cumulative distributions of ODI values) (E) Cumulative distributions of ODIs of individual units after 8 days of binocular vision. *Ngr1–/–* mice exhibited greater OD plasticity resulting in greater contralateral bias than WT mice (WT vs. *ngr1–/–*, $P < 0.001$, K–S test of Day 8 cumulative distributions).

important and extensive similarities between the experiments presented here and those published by Akbik et al., we are confident we would have detected the dramatic increase in cortical anatomical plasticity proposed by Strittmatter and colleagues if the findings they reported reflect the function of *ngr1* in cortical pyramidal neurons expressing the gene.

LTMD is a murine model of amblyopia that induces a permanent deficit in visual acuity in WT mice. Visual acuity spontaneously improves to almost normal over 7 weeks in *ngr1–/–* mice following LTMD (Stephany et al. 2014). To determine whether the restoration of vision following LTMD alters axonal plasticity in visual cortex, we again examined the turnover of axonal boutons in layer I with chronic two-photon in vivo imaging (Fig. 3). Re-opening the deprived eye did not alter the rate of bouton gain in either WT or *ngr1–/–* mice but did increase the variability in the rate of bouton loss for both genotypes. Thus, anatomical plasticity by intracortical axons in layer I during the first week of normal vision post-LTMD did not correlate with the eventual improvement of acuity we observe in *ngr1–/–* mutant mice. However, length and branching patterns of thalamocortical axons are

altered by LTMD (Antonini et al. 1999). Anatomical plasticity by these projections mediates the changes in OD columns present in predatory mammals following similar visual deprivation (LeVay et al. 1980). Future studies will be required to determine whether plasticity by this population of axons differs between WT and *ngr1–/–* mice following LTMD.

Given this disparity between axonal and dendritic structural plasticity during MD, we propose that cortical anatomical plasticity in response to durations of abnormal visual experience is predominantly postsynaptic in origin and that new spines preferentially form synaptic contacts with preexisting axonal boutons. This model is supported by evidence that newly formed spines contact boutons with other synapses (Knott et al. 2006). However, several alternative interpretations are consistent with the results presented here and cannot be excluded from consideration. Foremost, new spines may form synaptic contacts on new boutons present on axons not examined here, such as thalamocortical axons. Projections from LGN send extensive collaterals into the supragranular layers, including layer I (Antonini et al. 1999). New spines may synapse selectively on these thalamic projections, or axons
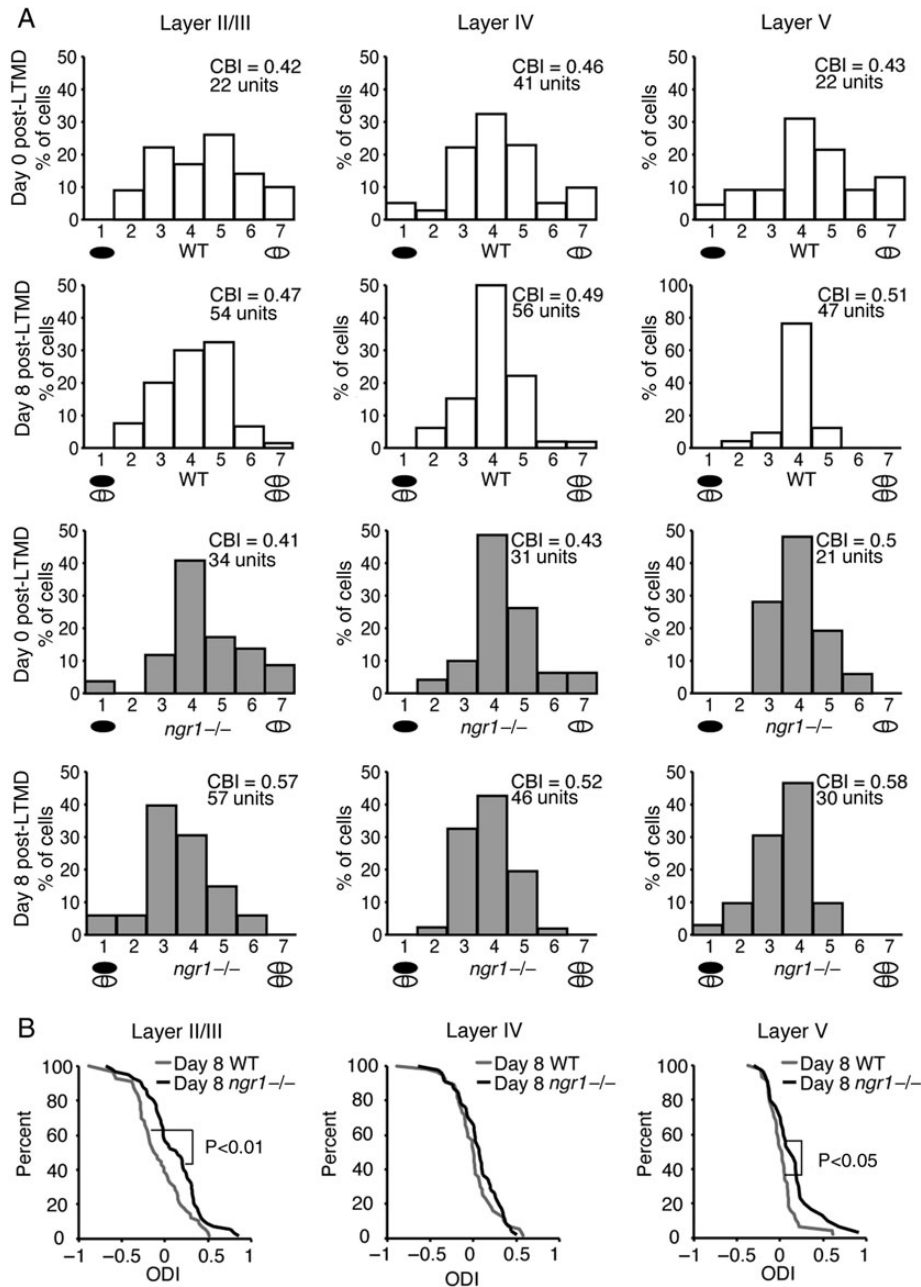
Figure 6. Laminar analysis of OD plasticity following LTMD (A) OD histograms of units from layer II/III (left), layer IV (center), and layer V (right) from WT and *ngr1−/−* mice either during LTMD (Day 0) or 8 days after re-opening the deprived eye. Cumulative distributions of ODIs for units from layer II/III (left), layer IV (center), and layer V (right) from WT and *ngr1−/−* mice after 8 days of normal vision through the deprived eye post-LTMD. (B) *Ngr1−/−* mice display greater overall contralateral bias in layer II/III (P < 0.01), and layer V (P < 0.05), but not in layer IV on Day 8 (P > 0.27) (K–S test of cumulative distributions of ODI values).

from layer VI neurons that are also evident in layer I (De Paola et al. 2006). In adult mice, sensory adaptation, motor learning, and fear conditioning are associated with elevated cortical spine dynamics (Trachtenberg et al. 2002; Holtmaat et al. 2006; Keck et al. 2008; Hofer et al. 2009; Xu et al. 2009; Wilbrecht et al. 2010; Yang et al. 2010; Lai et al. 2013). New spines associated with motor learning, tone-associated fear conditioning, and fear extinction may also preferentially form synapses on preexisting stable intracortical axonal boutons (Yang et al. 2010; Lai et al. 2013).

Reopening the deprived eye following LTMD yielded a surprising restoration of normal contralateral bias as reflected by OIS (Fig. 4). We employed an established technique for examining OD plasticity with OIS (Cang et al. 2005; Kaneko, Hanover, et al. 2008; Kaneko, Stellwagen, et al. 2008; Sato and Stryker 2008; Kaneko et al. 2010; Sato and Stryker 2010; Southwell et al. 2010). Here, mice received LTMD from P23, near the beginning of the critical period, for 6 weeks (P23–P60+) and were then imaged repeatedly on the day of eye opening (Day 0) and then at Days 2, 4, and 8 thereafter. By 8 days following restoration of normal vision, both WT and *ngr1−/−* mice displayed normal contralateral bias as revealed by ODI scores near 0.2.

OIS likely represents a combination of both subthreshold and suprathreshold neuronal responses, although the magnitude of response is correlated with firing activity in some studies

(Hofer et al. 2006; Kaneko, Stellwagen, et al. 2008). Similar experiments examining VEPs have not detected similar OD plasticity with binocular vision following chronic deprivation (He et al. 2007). However, in this latter study, rats received a more extensive LTMD from eye opening to adulthood (P70–100). As experience-dependent plasticity in visual cortex begins at eye opening (Smith and Trachtenberg 2007), perhaps the absence of patterned vision by the deprived eye contributes to these differing results.

LTMD results in a permanent shift in OD in WT mice. To determine whether the recovery of contralateral bias we observed with OIS reflected spike-related output changes in visual cortex, we examined both WT and *ngr1*–/– mice following eye-opening under anesthesia as well as after 8 days of binocular vision (Fig. 5). OD plasticity is normal during the critical period in *ngr1*–/– mice, but unlike WT mice, this developmental visual plasticity is retained into adulthood (McGee et al. 2005). We observed that *ngr1*–/– displayed significantly greater OD plasticity that WT mice. On Day 8 following LTMD, *ngr1*–/– mice exhibited nearly twice the recovery of contralateral bias as WT mice. However, OD remained more binocular than nondeprived mice. This OD plasticity precedes improvement of visual acuity in *ngr1*–/– mice because WT and *ngr1*–/– mice possess similar deficits in acuity 7 days after LTMD (Stephany et al. 2014). Categorizing these single-unit recordings into cortical layers by depth from the pial surface revealed that OD plasticity was evident in the extragranular layers II/III and V.

In summary, as *ngr1*–/– mice display a greater restoration of normal eye dominance than WT mice as measured with single-unit recordings following LTMD, we propose that *ngr1* limits recovery of cortical responsiveness in a murine model of amblyopia but does not restrict axonal plasticity in visual cortex.

Authors' Contributions

Aaron W. McGee and Michael G. Frantz designed the study and wrote the manuscript. Aaron W. McGee supervised all experiments; Michael G. Frantz performed chronic in vivo imaging and analysis of cortical bouton dynamics; Ryan J. Kast, Katherine S. Chapman, and Hilary M. Dorton assisted with analysis of bouton turnover and stability; and Michael G. Frantz performed in the OIS imaging and also performed electrophysiological recordings with assistance from KSC.

Funding

Notes

Conflict of Interest: None declared.

References

Akbik FV, Bhagat SM, Patel PR, Cafferty WBJ, Strittmatter SM. 2013. Anatomical plasticity of adult brain is titrated by Nogo receptor 1. Neuron. 77:859–866.

Antonini A, Fagiolini M, Stryker MP. 1999. Anatomical correlates of functional plasticity in mouse visual cortex. J Neurosci. 19:4388–4406.

Cang J, Kalatsky VA, Löwel S, Stryker MP. 2005. Optical imaging of the intrinsic signal as a measure of cortical plasticity in the mouse. Vis Neurosci. 22:685–691.

Coleman JE, Nahmani M, Gavornik JP, Haslinger R, Heynen AJ, Erisir A, Bear MF. 2010. Rapid structural remodeling of thalamocortical synapses parallels experience-dependent functional plasticity in mouse primary visual cortex. J Neurosci. 30:9670–9682.

Debanne D, Campanac E, Bialowas A, Carlier E, Alcaraz G. 2011. Axon physiology. Physiol Rev. 91:555–602.

De Paola V, Holtmaat A, Knott G, Song S, Wilbrecht L, Caroni P, Svoboda K. 2006. Cell type-specific structural plasticity of axonal branches and boutons in the adult neocortex. Neuron. 49:861–875.

Djurisic M, Vidal GS, Mann M, Aharon A, Kim T, Ferrao Santos A, Zuo Y, Hübener M, Shatz CJ. 2013. PirB regulates a structural substrate for cortical plasticity. Proc Natl Acad Sci. 110:20771–20776.

Douglas RJ, Martin KAC. 2004. Neuronal circuits of the neocortex. Annu Rev Neurosci. 27:419–451.

Feng G, Mellor RH, Bernstein M, Keller-Peck C, Nguyen QT, Wallace M, Nerbonne JM, Lichtman JW, Sanes JR. 2000. Imaging neuronal subsets in transgenic mice expressing multiple spectral variants of GFP. Neuron. 28:41–51.

Filbin MT. 2008. PirB, a second receptor for the myelin inhibitors of axonal regeneration Nogo66, MAG, and OMgp: implications for regeneration in vivo. Neuron. 60:740–742.

Fischer QS, Graves A, Evans S, Lickey ME, Pham TA. 2007. Monocular deprivation in adult mice alters visual acuity and single-unit activity. Learn Mem. 14:277–286.

Frenkel MY, Bear MF. 2004. How monocular deprivation shifts ocular dominance in visual cortex of young mice. Neuron. 44:917–923.

Gordon JA, Stryker MP. 1996. Experience-dependent plasticity of binocular responses in the primary visual cortex of the mouse. J Neurosci. 16:3274–3286.

He H-Y, Ray B, Dennis K, Quinlan EM. 2007. Experience-dependent recovery of vision following chronic deprivation amblyopia. Nat Neurosci. 10:1134–1136.

Hofer SB, Mrsic-Flogel TD, Bonhoeffer T, Hübener M. 2006. Prior experience enhances plasticity in adult visual cortex. Nat Neurosci. 9:127–132.

Hofer SB, Mrsic-Flogel TD, Bonhoeffer T, Hübener M. 2009. Experience leaves a lasting structural trace in cortical circuits. Nature. 457:313–317.

Holtmaat A, Bonhoeffer T, Chow DK, Chuckowree J, De Paola V, Hofer SB, Hübener M, Keck T, Knott G, Lee W-CA, et al. 2009. Long-term, high-resolution imaging in the mouse neocortex through a chronic cranial window. Nat Protoc. 4:1128–1144.

Holtmaat A, Svoboda K. 2009. Experience-dependent structural synaptic plasticity in the mammalian brain. Nat Rev Neurosci. 10:647–658.

Holtmaat A, Wilbrecht L, Knott GW, Welker E, Svoboda K. 2006. Experience-dependent and cell-type-specific spine growth in the neocortex. Nature. 441:979–983.

Kalatsky VA, Polley DB, Merzenich MM, Schreiner CE, Stryker MP. 2005. Fine functional organization of auditory cortex revealed by Fourier optical imaging. Proc Natl Acad Sci USA. 102:13325–13330.

Kalatsky VA, Stryker MP. 2003. New paradigm for optical imaging: temporally encoded maps of intrinsic signal. Neuron. 38:529–545.

Kaneko M, Cheetham CE, Lee Y-S, Silva AJ, Stryker MP, Fox K. 2010. Constitutively active H-ras accelerates multiple forms of plasticity in developing visual cortex. Proc Natl Acad Sci. 107:19026–19031.

Kaneko M, Hanover JL, England PM, Stryker MP. 2008. TrkB kinase is required for recovery, but not loss, of cortical responses following monocular deprivation. Nat Neurosci. 11:497–504.

Kaneko M, Stellwagen D, Malenka RC, Stryker MP. 2008. Tumor necrosis factor-alpha mediates one component of competitive, experience-dependent plasticity in developing visual cortex. Neuron. 58:673–680.

Keck T, Mrsic-Flogel TD, Vaz Afonso M, Eysel UT, Bonhoeffer T, Hübener M. 2008. Massive restructuring of neuronal circuits during functional reorganization of adult visual cortex. Nat Neurosci. 11:1162–1167.

Kim J-E, Liu BP, Park JH, Strittmatter SM. 2004. Nogo-66 receptor prevents raphespinal and rubrospinal axon regeneration and limits functional recovery from spinal cord injury. Neuron. 44:439–451.

Knott GW, Holtmaat A, Wilbrecht L, Welker E, Svoboda K. 2006. Spine growth precedes synapse formation in the adult neocortex in vivo. Nat Neurosci. 9:1117–1124.

Lai CSW, Franke TF, Gan W-B. 2013. Opposite effects of fear conditioning and extinction on dendritic spine remodelling. Nature. 482:87–91.

LeVay S, Wiesel TN, Hubel DH. 1980. The development of ocular dominance columns in normal and visually deprived monkeys. J Comp Neurol. 191:1–51.

Levelt CN, Hübener M. 2012. Critical-period plasticity in the visual cortex. Annu Rev Neurosci. 35:309–330.

Mataga N, Mizuguchi Y, Hensch TK. 2004. Experience-dependent pruning of dendritic spines in visual cortex by tissue plasminogen activator. Neuron. 44:1031–1041.

McGee AW, Yang Y, Fischer QS, Daw NW, Strittmatter SM. 2005. Experience-driven plasticity of visual cortex limited by myelin and Nogo receptor. Science. 309:2222–2226.

Mironova YA, Giger RJ. 2013. Where no synapses go: gatekeepers of circuit remodeling and synaptic strength. Trends Neurosci. 36:363–373.

Mitchell DE, Sengpiel F. 2009. Neural mechanisms of recovery following early visual deprivation. Philos Trans R Soc Lond B Biol Sci. 364:383–398.

Montey KL, Quinlan EM. 2011. Recovery from chronic monocular deprivation following reactivation of thalamocortical plasticity by dark exposure. Nat Commun. 2:317–318.

Morishita H, Hensch TK. 2008. Critical period revisited: impact on vision. Curr Opin Neurobiol. 18:101–107.

Park JI, Frantz MG, Kast RJ, Chapman KS, Dorton HM, Stephany C-É, Arnett MT, Herman DH, McGee AW. 2014.

Nogo receptor 1 limits tactile task performance independent of basal anatomical plasticity. PLoS ONE. 9:e112678.

Pologruto TA, Sabatini BL, Svoboda K. 2003. ScanImage: flexible software for operating laser scanning microscopes. BioMed Eng OnLine. 2:13.

Prusky GT, Douglas RM. 2003. Developmental plasticity of mouse visual acuity. Eur J Neurosci. 17:167–173.

Rittenhouse CD, Shouval HZ, Paradiso MA, Bear MF. 1999. Monocular deprivation induces homosynaptic long-term depression in visual cortex. Nature. 397:347–350.

Sala C, Segal M. 2014. Dendritic spines: the locus of structural and functional plasticity. Physiol Rev. 94:141–188.

Sato M, Stryker MP. 2008. Distinctive features of adult ocular dominance plasticity. J Neurosci. 28:10278–10286.

Sato M, Stryker MP. 2010. Genomic imprinting of experience-dependent cortical plasticity by the ubiquitin ligase gene Ube3a. Proc Natl Acad Sci. 107:5611–5616.

Sawtell NB, Frenkel MY, Philpot BD, Nakazawa K, Tonegawa S, Bear MF. 2003. NMDA receptor-dependent ocular dominance plasticity in adult visual cortex. Neuron. 38:977–985.

Schwarzkopf DS, Vorobyov V, Mitchell DE, Sengpiel F. 2007. Brief daily binocular vision prevents monocular deprivation effects in visual cortex. Eur J Neurosci. 25:270–280.

Smith SL, Trachtenberg JT. 2007. Experience-dependent binocular competition in the visual cortex begins at eye opening. Nat Neurosci. 10:370–375.

Southwell DG, Froemke RC, Alvarez-Buylla A, Stryker MP, Gandhi SP. 2010. Cortical plasticity induced by inhibitory neuron transplantation. Science. 327:1145–1148.

Stephany CE, Chan LLH, Parivash SN, Dorton HM, Piechowicz M, Qiu S, McGee AW. 2014. Plasticity of Binocularity and Visual Acuity Are Differentially Limited by Nogo Receptor. J Neurosci. 34:11631–11640.

Trachtenberg JT, Chen BE, Knott GW, Feng G, Sanes JR, Welker E, Svoboda K. 2002. Long-term in vivo imaging of experience-dependent synaptic plasticity in adult cortex. Nature. 420:788–794.

Wiesel TN, Hubel DH. 1963. Single-cell responses in striate cortex of kittens deprived of vision in one eye. J Neurophysiol. 26:1003–1017.

Wilbrecht L, Holtmaat A, Wright N, Fox K, Svoboda K. 2010. Structural plasticity underlies experience-dependent functional plasticity of cortical circuits. J Neurosci. 30:4927–4932.

Xu T, Yu X, Perlik AJ, Tobin WF, Zweig JA, Tennant K, Jones T, Zuo Y. 2009. Rapid formation and selective stabilization of synapses for enduring motor memories. Nature. 462:915–919.

Yang G, Pan F, Gan W-B. 2010. Stably maintained dendritic spines are associated with lifelong memories. Nature. 462:920–924.